AMERICAN SOCIETY FOR MICROBIOLOGY | Antimicrobial Agents and Chemotherapy®

ANTIVIRAL AGENTS

# Halogen Bond Interactions of Novel HIV-1 Protease Inhibitors (PI) (GRL-001-15 and GRL-003-15) with the Flap of Protease Are Critical for Their Potent Activity against Wild-Type HIV-1 and Multi-PI-Resistant Variants

**Shin-ichiro Hattori,[a] Hironori Hayashi,[a]* Haydar Bulut,[b] Kalapala Venkateswara Rao,[c,d] Prasanth R. Nyalapatla,[c,d] Kazuya Hasegawa,[e] Manabu Aoki,[a,b] Arun K. Ghosh,[c,d] Hiroaki Mitsuya[a,b,f]**

[a]Department of Refractory Viral Infections, National Center for Global Health and Medicine Research Institute, Tokyo, Japan
[b]Experimental Retrovirology Section, HIV and AIDS Malignancy Branch, National Cancer Institute, National Institutes of Health, Bethesda, Maryland, USA
[c]Department of Chemistry, Purdue University, West Lafayette, Indiana, USA
[d]Department of Medicinal Chemistry, Purdue University, West Lafayette, Indiana, USA
[e]Protein Crystal Analysis Division, Japan Synchrotron Radiation Research Institute, Hyogo, Japan
[f]Department of Clinical Sciences, Kumamoto University Hospital, Kumamoto, Japan

**ABSTRACT** We generated two novel nonpeptidic HIV-1 protease inhibitors (PIs), GRL-001-15 and GRL-003-15, which contain unique crown-like tetrahydropyranofuran (Crn-THF) and P2′-cyclopropyl-aminobenzothiazole (Cp-Abt) moieties as P2 and P2′ ligands, respectively. GRL-001-15 and GRL-003-15 have *meta*-monofluorophenyl and *para*-monofluorophenyl at the P1 site, respectively, exert highly potent activity against wild-type HIV-1 with 50% effective concentrations ($EC_{50}$s) of 57 and 50 pM, respectively, and have favorable cytotoxicity profiles with 50% cytotoxic concentrations ($CC_{50}$s) of 38 and 11 $\mu$M, respectively. The activity of GRL-001-15 against multi-PI-resistant HIV-1 variants was generally greater than that of GRL-003-15. The $EC_{50}$ of GRL-001-15 against an HIV-1 variant that was highly resistant to multiple PIs, including darunavir (DRV) (HIV-$1_{DRV}{}^{R}{}_{P30}$), was 0.17 nM, and that of GRL-003-15 was 3.3 nM, while DRV was much less active, with an $EC_{50}$ of 216 nM. The emergence of HIV-1 variants resistant to GRL-001-15 and GRL-003-15 was significantly delayed compared to that of variants resistant to selected PIs, including DRV. Structural analyses of wild-type protease ($PR^{WT}$) complexed with the novel PIs revealed that GRL-001-15's *meta*-fluorine atom forms halogen bond interactions (2.9 and 3.0 Å) with Gly49 and Ile50, respectively, of the protease flap region and with Pro81′ (2.7 and 3.2 Å), which is located close to the protease active site, and that two fluorine atoms of GRL-142-13 form multiple halogen bond interactions with Gly49, Ile50, Pro81′, Ile82′, and Arg8′. In contrast, GRL-003-15 forms halogen bond interactions with Pro81′ alone, suggesting that the reduced antiviral activity of GRL-003-15 is due to the loss of the interactions with the flap region.

**KEYWORDS** AIDS, HIV-1, antiretroviral therapy, protease inhibitors

Human immunodeficiency virus type 1 (HIV-1) infection and AIDS have now been well controlled, and the expected life span of people with HIV has been significantly extended in both developing and developed countries by presently available combination antiretroviral therapy (cART) (1–4). Indeed, cART has been shown not only to significantly reduce the mortality and morbidity rates for people with HIV-1 but also to prevent sexual transmission of HIV-1 by 93 to 96% (5, 6). Yet, at the end of 2017, the number of people living with HIV was reportedly 36.9 million, and the numbers of people newly infected with HIV and the lives lost due to HIV/AIDS in 2017 were 1.8

**Citation** Hattori S-I, Hayashi H, Bulut H, Rao KV, Nyalapatla PR, Hasegawa K, Aoki M, Ghosh AK, Mitsuya H. 2019. Halogen bond interactions of novel HIV-1 protease inhibitors (PI) (GRL-001-15 and GRL-003-15) with the flap of protease are critical for their potent activity against wild-type HIV-1 and multi-PI-resistant variants. Antimicrob Agents Chemother 63:e02635-18. https://doi.org/10.1128/AAC.02635-18.



Address correspondence to Hiroaki Mitsuya, hiroaki.mitsuya2@nih.gov.

* Present address: Hironori Hayashi, Department of Intelligent Network for Infection Control, Tohoku University Graduate School of Medicine, Miyagi, Japan.

**Received** 3 January 2019
**Returned for modification** 4 February 2019
**Accepted** 3 April 2019
**Accepted manuscript posted online** 8 April 2019
**Published** 24 May 2019

million and 0.94 million, respectively (7). Moreover, the cure of HIV-1/AIDS is still elusive (8). In addition, our capability to provide effective long-term cART remains a complex issue, since many of those who initially achieve favorable viral suppression to undetectable levels eventually suffer treatment failure. Nevertheless, regarding to the propensity of HIV-1 to acquire resistance to antiretroviral agents, protease inhibitors (PIs) generally have been known to have a high genetic barrier against the emergence of drug resistance (9, 10). In particular, the latest FDA-approved PI, darunavir (DRV), which is widely used and was recommended as one of the initial regimens in certain clinical situations in the 2018 U.S. Department of Health and Human Services guidelines (11), has a favorable genetic barrier, probably because of its dual mechanism of action: (i) inhibition of protease enzymatic activity and (ii) inhibition of protease dimerization (12–14). Yet, the emergence of DRV-resistant HIV-1 variants has been reported both *in vitro* and *in vivo*, and people with such DRV-resistant HIV-1 variants experience treatment failure (15–17). Furthermore, 12 to 21% of individuals receiving DRV-containing regimens discontinue the treatment due to adverse events, diarrhea, and virological failure (18–20). Dolutegravir (DTG), an integrase strand transfer inhibitor (INSTI), is also widely used and recommended as the first-line drug in most people with HIV-1 (11). However, serious adverse events such as gastrointestinal disorders and various central nervous system abnormalities have been reported in people receiving DTG (21, 22). Moreover, DTG treatment at the time of conception is highly associated with neural tube defects in infants, and multiple warnings have been issued that women living with HIV-1 who can become pregnant should not use DTG without effective contraception (23). Thus, the development of novel antiretroviral agents with better features, such as greater potency against both wild-type HIV-1 ($HIV_{WT}$) and drug-resistant HIV-1 variants, a higher genetic barrier against HIV-1's development of drug resistance, and minimal or no adverse effects, is still needed.

In the present work, we designed, synthesized, and characterized two novel nonpeptidic HIV-1 PIs, GRL-001-15 and GRL-003-15, that are analogues of GRL-142-13, which we previously reported (24). Each compound contains a P2-crown-like tetrahydropyranofuran (Crn-THF) functional moiety (25), a P2′-cyclopropyl-aminobenzothiazole (Cp-Abt) moiety, and *meta*- or *para*-monofluorophenyl at the P1 site. Here, we show that the two novel PIs exhibit highly favorable antiretroviral profiles against wild-type $HIV_{NL4-3}$ and multidrug-resistant HIV-1 variants ($HIV_{MDR}$s). We also demonstrate that those PIs have very high genetic barriers when selected using $HIV_{DRV}{}^{R}{}_{P30}$, which is an *in vitro*-selected highly DRV-resistant HIV-1 variant, as a starting viral population. We also demonstrate the results of structural analyses of the atomic and molecular interactions of GRL-001-15 and GRL-003-15 with HIV-1 protease.

## RESULTS

**GRL-001-15 and GRL-003-15 are potent against wild-type HIV-1 and have favorable cytotoxic profiles.** We newly designed and synthesized two novel PIs, GRL-001-15 and GRL-003-15, which contain unique P2-crown-THF (Crn-THF) and P2′-cyclopropyl-aminobenzothiazole (Cp-Abt) moieties (Fig. 1). GRL-001-15 and GRL-003-15 have a fluorine atom at the *meta* and *para* positions of the P1-benzene, respectively, and exerted highly potent activity against the wild-type HIV-1 NL4-3 strain ($HIV_{NL4-3}$), with 50% effective concentration ($EC_{50}$) values of 0.057 $\pm$ 0.0024 nM and 0.050 $\pm$ 0.025 nM, respectively (Table 1). Two other PIs, GRL-142-13 (containing two fluorine atoms at the P1-2,4-*meta* position) and GRL-121-13 (containing no fluorine atoms) (Fig. 1) (24–26), which served as reference compounds in the present study and contain P2-Crn-THF and P2′-Cp-Abt, respectively, also exerted potent activity against $HIV_{NL4-3}$, with $EC_{50}$ values of 0.018 $\pm$ 0.0014 and 0.17 $\pm$ 0.12 nM, respectively (Table 1). When human CD4-positive MT-4 cells were exposed to GRL-001-15 and GRL-003-15 for 7 days and their cytotoxicity profiles were determined, their 50% cytotoxic concentrations ($CC_{50}$s) proved to be relatively favorable at 38 and 11 $\mu$M, respectively, and their selectivity indexes were 666,666 and 220,000, respectively, much greater than that of DRV, whose selectivity index was 45,121 (Table 1).

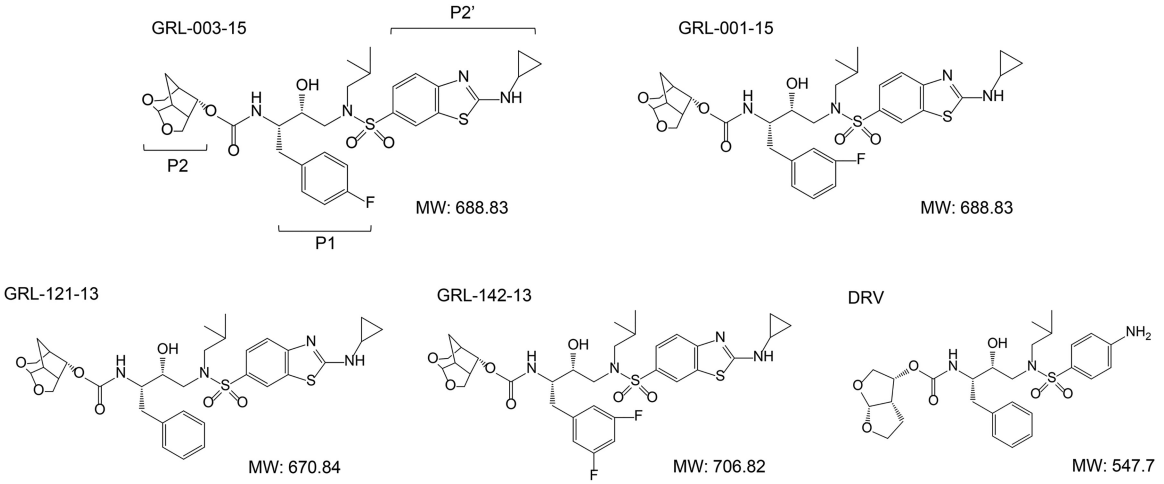


**FIG 1** Structures of protease inhibitors examined. MW, molecular weight.

**GRL-001-15 and GRL-003-15 exert potent activity against laboratory-selected and clinically isolated PI-resistant HIV-1 variants.** We next examined whether GRL-001-15 and GRL-003-15 were active against various laboratory-selected PI-resistant HIV variants ($_{lab}HIV_{PI}^{R}$s) that had been selected with the FDA-approved PIs saquinavir (SQV), amprenavir (APV), lopinavir (LPV), indinavir (IDV), nelfinavir (NFV), atazanavir (ATV), and tipranavir (TPV) ($HIV_{SQV\text{-}5\mu M}$, $HIV_{APV\text{-}5\mu M}$, $HIV_{LPV\text{-}5\mu M}$, $HIV_{IDV\text{-}5\mu M}$, $HIV_{NFV\text{-}5\mu M}$, $HIV_{ATV\text{-}5\mu M}$, and $HIV_{TPV\text{-}15\mu M}$, respectively) as previously reported (24, 25). They had a variety of amino acid substitutions in protease that are reportedly associated with the acquisition of resistance against PIs (see Fig. S1 in the supplemental material). Although DRV exerted moderate activity against the seven $_{lab}HIV_{PI}^{R}$s, with 50% effective concentration ($EC_{50}$) values ranging from 5.1 to 346 nM, GRL-001-15 and GRL-003-15 exerted much more potent activity against all the $_{lab}HIV_{PI}^{R}$s, with $EC_{50}$ values of 0.00019 to 0.37 nM (Table 2). GRL-121-13 was also potent against all seven $_{lab}HIV_{PI}^{R}$s, with $EC_{50}$ values ranging from 0.0022 to 0.087 nM (Table 2). DRV proved to be comparatively less potent against the three $HIV_{DRV}^{R}$s ($HIV_{DRV}^{R}{}_{P20}$, $HIV_{DRV}^{R}{}_{P30}$, and $HIV_{DRV}^{R}{}_{P51}$) (Fig. S1), with $EC_{50}$ values ranging from 81 to 2,707 nM, in line with our previous reports (16, 24). However, GRL-001-15 and GRL-003-15 maintained their potent activity against the three $HIV_{DRV}^{R}$s, with $EC_{50}$ values of 0.17 to 38 nM (Table 2). GRL-121-13 was also relatively potent against those $HIV_{DRV}^{R}$s but was less potent than GRL-001-15 and GRL-003-15, with $EC_{50}$ values ranging from 4.3 to 99 nM. Moreover, all three compounds, GRL-001-15, GRL-003-15, and GRL-121-13, exerted greater antiviral activity against all of the PI-resistant HIV strains examined than DRV (see Table S2 in the supplemental material).

We further examined GRL-001-15 and GRL-003-15 against six recombinant infectious clones derived from clinically isolated HIV variants ($_{rCL}$HIVs) that contained multi-PI resistance-associated amino acid substitutions in their proteases (24) (Fig. S1). DRV was

**TABLE 1** *In vitro* antiviral activity of GRL-001-15 and GRL-003-15 against $HIV_{NL4\text{-}3}$ and their cytotoxic profiles

| PI | $EC_{50}$ (nM)[a] | $CC_{50}$ ($\mu$M)[a] | Selectivity index[b] |
|---|---|---|---|
| DRV | 4.1 ± 1.3 | 185 ± 8.4 | 45,121 |
| GRL-003-15 | 0.050 ± 0.025 | 11 ± 0.9 | 220,000 |
| GRL-001-15 | 0.057 ± 0.0024 | 38 ± 0.8 | 666,666 |
| GRL-121-13 | 0.17 ± 0.12 | 23 ± 2.9 | 135,294 |
| GRL-142-13 | 0.018 ± 0.0014 | 32 ± 1.6 | 1,777,777 |

[a]All assays were conducted in duplicate, and the data shown represent mean values (±1 standard deviation) derived from the results of at least three independent experiments.
[b]The selectivity index is the ratio of the $CC_{50}$ to the $EC_{50}$.

**TABLE 2** Antiviral effects against selected PI-resistant HIV-1 variants and recombinant clinical HIV-1 isolates

| HIV strain[a] | Mean $EC_{50}$[b] | | | |
|---|---|---|---|---|
| | DRV | GRL-003-15 | GRL-001-15 | GRL-121-13 |
| $HIV_{NL4-3}$ | 3.0 ± 0.3 | 0.049 ± 0.02 | 0.061 ± 0.008 | 0.30 ± 0.02 |
| $HIV_{SQV-5\mu M}$ | 29 ± 17 (10) | 0.0032 ± 0.0002 (0.06) | 0.37 ± 0.05 (6) | 0.015 ± 0.02 (0.05) |
| $HIV_{APV-5\mu M}$ | 98 ± 83 (33) | 0.0021 ± 0.0001 (0.04) | 0.00068 ± 0.00009 (0.01) | 0.068 ± 0.09 (0.2) |
| $HIV_{LPV-5\mu M}$ | 346 ± 93 (115) | 0.00015 ± 0.00001 (0.003) | 0.0040 ± 0.0005 (0.07) | 0.0022 ± 0.0006 (0.007) |
| $HIV_{IDV-5\mu M}$ | 22 ± 2 (7) | 0.00037 ± 0.00002 (0.007) | 0.00020 ± 0.00003 (0.003) | 0.0056 ± 0.005 (0.02) |
| $HIV_{NFV-5\mu M}$ | 5.1 ± 3.7 (2) | 0.00089 ± 0.0001 (0.02) | 0.00019 ± 0.0001 (0.03) | 0.024 ± 0.03 (0.08) |
| $HIV_{ATV-5\mu M}$ | 24 ± 1 (8) | 0.00084 ± 0.0001 (0.02) | 0.0020 ± 0.001 (0.03) | 0.046 ± 0.07 (0.2) |
| $HIV_{TPV-15\mu M}$ | 29 ± 16 (10) | 0.0005 ± 0.00004 (0.01) | 0.057 ± 0.007 (0.9) | 0.087 ± 0.03 (0.3) |
| $HIV_{DRV}{}^{R}{}_{P20}$ | 81 ± 4 (27) | 2.2 ± 0.1 (45) | 0.37 ± 0.04 (6) | 4.3 ± 1 (14) |
| $HIV_{DRV}{}^{R}{}_{P30}$ | 216 ± 9 (72) | 3.3 ± 0.2 (66) | 0.17 ± 0.02 (3) | 23 ± 0.4 (77) |
| $HIV_{DRV}{}^{R}{}_{P51}$ | 2707 ± 13 (902) | 38 ± 3 (771) | 36 ± 4 (594) | 99 ± 13 (330) |
| $_{rCL}HIV_{F16}$ | 2498 ± 122 (833) | 0.00063 ± 0.00004 (0.01) | 0.00044 ± 0.00005 (0.01) | 2.0 ± 0.7 (7) |
| $_{rCL}HIV_{F39}$ | 322 ± 13 (107) | 3.6 ± 0.2 (73) | 3.6 ± 0.5 (60) | 4.3 ± 0.7 (14) |
| $_{rCL}HIV_{V42}$ | 371 ± 39 (124) | 3.9 ± 0.3 (79) | 4.3 ± 0.6 (71) | 16 ± 6 (53) |
| $_{rCL}HIV_{T45}$ | 190 ± 20 (63) | 3.6 ± 0.2 (73) | 3.6 ± 0.5 (60) | 3.3 ± 0.2 (11) |
| $_{rCL}HIV_{T48}$ | 324 ± 12 (108) | 0.034 ± 0.002 (0.7) | 0.37 ± 0.05 (6) | 0.61 ± 0.5 (2) |
| $_{rCL}HIV_{F71}$ | 332 ± 45 (111) | 3.9 ± 0.3 (79) | 4.1 ± 0.5 (67) | 17 ± 8 (57) |

[a]The amino acid substitutions identified in the proteases of laboratory-selected FDA-approved HIV variants ($HIV_{SQV-5\mu M}$, $HIV_{APV-5\mu M}$, $HIV_{LPV-5\mu M}$, $HIV_{IDV-5\mu M}$, $HIV_{NFV-5\mu M}$, $HIV_{ATV-5\mu M}$, and $HIV_{TPV-15\mu M}$ and the $HIV_{DRV}{}^{R}$s $HIV_{DRV}{}^{R}{}_{P20}$, $HIV_{DRV}{}^{R}{}_{P30}$, and $HIV_{DRV}{}^{R}{}_{P51}$) and recombinant clinical HIV isolates ($_{rCL}HIV_{F16}$, $_{rCL}HIV_{F39}$, $_{rCL}HIV_{V42}$, $_{rCL}HIV_{T45}$, $_{rCL}HIV_{T48}$, and $_{rCL}HIV_{F71}$) compared to the wild-type $HIV_{NL4-3}$ are illustrated in Fig. S1 in the supplemental material.

[b]Numbers in parentheses represent the fold change in the $EC_{50}$ for each isolate compared to the $EC_{50}$ for wild-type $HIV_{NL4-3}$. All assays were conducted in duplicate, and the data shown represent mean values (± 1 standard deviation) derived from the results of three independent experiments.

found to have greatly reduced activity against such $_{rCL}$HIVs, with $EC_{50}$s ranging from 190 to 2,498 nM, whereas GRL-003-15 and GRL-001-15 maintained their potent activity against the $_{rCL}$HIVs, with $EC_{50}$ values of 0.00044 to 4.3 nM (Tables 2 and S2). Compared to GRL-001-15 and GRL-003-15, GRL-121-13 was less potent against the $_{rCL}$HIVs, with $EC_{50}$ values ranging from 0.61 to 17 nM (Table 2).

**GRL-001-15 and GRL-003-15 tightly bind to protease as assessed by DSF.** We then examined if the two PIs, GRL-003-15 and GRL-001-15, bound to HIV-1 protease containing the amino acid substitution D25N ($PR^{D25N}$) by differential scanning fluorimetry (DSF) employing the dye Sypro Orange (12, 24, 27). As illustrated in Fig. 2, the melting temperature ($T_m$) of $PR^{D25N}$ alone was 54.8 ± 0.7°C, while in the presence of DRV, the value increased to 58.2 ± 0.3°C, suggesting that the thermal stability of $PR^{D25N}$ increased when DRV bound to $PR^{D25N}$. However, in the presence of GRL-001-15 and GRL-003-15, the $T_m$ values of $PR^{D25N}$ turned out to be substantially greater, at

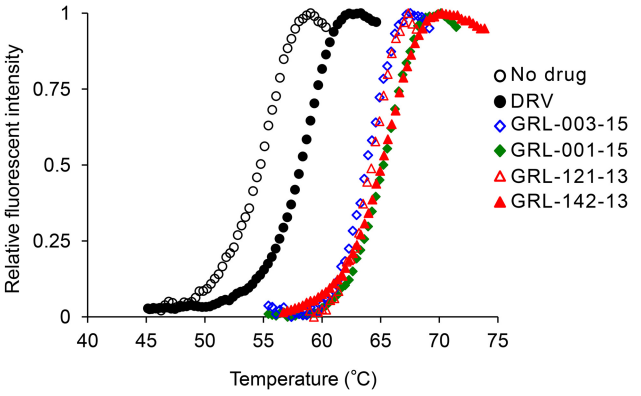


| Compounds | $T_m$ (°C) ($\Delta T_m$) $PR^{D25N}$ |
|---|---|
| No drug | 54.8 ± 0.7 |
| DRV | 58.2 ± 0.3 (3.4) |
| GRL-003-15 | 63.9 ± 0.4 (9.1) |
| GRL-001-15 | 65.2 ± 0.4 (10.4) |
| GRL-121-13 | 64.0 ± 0.3 (9.2) |
| GRL-142-13 | 65.7 ± 0.6 (10.9) |

**FIG 2** GRL-003-15 and GRL-001-15 bind to HIV-1 $PR^{D25N}$ and have much greater thermal stability than DRV. The thermal stability of $PR^{D25N}$ in the absence or presence of GRL-003-15, GRL-001-15, GRL-142-13, GRL-121-13, and DRV (all at 50 $\mu$M) was determined using differential scanning fluorimetry with Sypro Orange. The $T_m$ (50% melting temperature) values were determined as the temperature at which the relative fluorescence intensity achieved 50% of the maximum intensity. Note that the thermal stability curves with GRL-003-15, GRL-001-15, GRL-121-13, and GRL-142-13 significantly shifted to a higher temperature (to the right), and the $T_m$ values with these agents were much higher than those without agents or with DRV.

65.2 ± 0.4°C and 63.9 ± 0.4°C, respectively; the differences in $T_m$ ($\Delta T_m$) values between $PR^{D25N}$ alone and GRL-001-15-bound $PR^{D25N}$ and GRL-003-15-bound $PR^{D25N}$ reached as high as 10.4°C and 9.1°C, respectively, suggesting that GRL-001-15 and GRL-003-15 bind to $PR^{D25N}$ more strongly than DRV does. Considering that GRL-121-13 and GRL-142-13 also tightly bound to $PR^{D25N}$, generating $T_m$ values of 64.0 ± 0.3°C ($\Delta T_m$ = 9.2) and 65.7 ± 0.6°C ($\Delta T_m$ = 10.9), respectively, all three fluorine-containing PIs (GRL-001-15, GRL-003-15, and GRL-142-13) and the nonfluorinated GRL-121-13 tightly bound to $PR^{D25N}$ compared to DRV (12, 24).

**GRL-001-15 and GRL-003-15 show slightly higher lipophilicity indexes than DRV for their partition and distribution coefficients.** We also determined the partition (log *P*) and distribution (log *D*) coefficients of GRL-001-15, GRL-003-15, GRL-121-13, and GRL-142-13 compared with those of DRV, hypothesizing that these compounds might have favorable lipophilicity, since the presence of a fluorine atom(s) in certain compounds often confers greater lipophilicity (28–30). In the assay, we employed an organic alcohol (1-octanol) and water for log *P* determination as well as Tris-buffered saline (pH 7.4) (TBS) and water for log *D* determination. The standard curve established was used as a reference, and drug concentrations determined for each compartment (1-octanol, water, and TBS) were quantified on a light spectrophotometer as previously described (31). GRL-003-15, GRL-001-15, and GRL-142-13 showed relatively high concentrations in the octanol lipid interface (1.6 $\mu$M, 1.5 $\mu$M, and 1.9 $\mu$M, respectively) compared to those of the two nonfluorinated PIs, GRL-121-13 and DRV (1.1 and 0.8 $\mu$M, respectively) (see Table S1 in the supplemental material).

The *bis*-fluorinated PI, GRL-142-13, proved to be the most lipophilic, with a log *D* value of −1.01, based on the assumption that the more negative the log *D* value is, the less lipophilic the substance is estimated to be (31). GRL-003-15 and GRL-001-15 showed log *D* values (−1.11 and −1.19, respectively) slightly lower than that of GRL-142-13 (−1.01). GRL-121-13 was found to have a log *D* value (−1.37) comparable to that of DRV (−1.48). Thus, as expected, the presence of one fluorine atom in GRL-003-15 and GRL-001-15 apparently conferred lipophilicity greater than that of the two nonfluorinated PIs.

**Structural analysis of the molecular interactions of GRL-003-15 and GRL-001-15 with protease.** In an attempt to examine the structural mechanism(s) of the potent activity against both wild-type HIV-1 ($HIV_{NL4-3}$) and various multi-PI-resistant HIV-1 variants, we conducted crystallographic analyses on wild-type protease ($PR^{WT}$) complexed with fluorinated GRL-003-15 or GRL-001-15 compared with nonfluorinated GRL-121-13. As illustrated in Fig. 3A, GRL-003-15 and GRL-001-15 have two moieties, P2-Crn-THF and P2′-Cp-Abt, that are larger than those of DRV (which has P2-*bis*-THF and P2′-aminobenzene moieties), in addition to two fluorine atoms attached to the P1-benzene ring. Thus, both GRL-003-15 and GRL-001-15 should occupy a larger space in the hydrophobic cavity within the dimerized protease. GRL-003-15 and GRL-001-15 form 11 direct and 2 water-mediated hydrogen bonds with protease (Fig. 3B). Notably, the majority of the hydrogen bonds seen with both compounds are formed with both subunits via the main chains of aspartate residues D29 and D30 and the side chain of aspartate residue D25. Additional water-mediated hydrogen bond interactions took place with the main-chain amino groups of the flap residues I50 and I50′. The nonfluorinated GRL-121-13 was also found to form hydrogen bond interactions as seen in the case of GRL-003-15 and GRL-001-15. When we focused on the possible role of fluorine atoms in GRL-003-15 and GRL-001-15, each fluorine was found to have critical effects on the interactions of the compound with $PR^{WT}$. As shown in Fig. 3C, the P1-*para*-positioned fluorine atom contained in the P1 site of GRL-003-15 formed halogen bond interactions with P81′ of $PR^{WT}$. GRL-001-15 also formed tight interactions between its P1-*meta*-positioned fluorine atom and two amino acid residues in the flap region of $PR^{WT}$, G49 and I50. In contrast, the nonfluorinated PI, GRL-121-13, which has the same chemical structure as in GRL-003-15 and GRL-001-15 but has no fluorine atom, does not form significant interactions between its P1-benzene moiety and $PR^{WT}$. These structural features of GRL-003-15 and GRL-001-15 should contribute to their potency

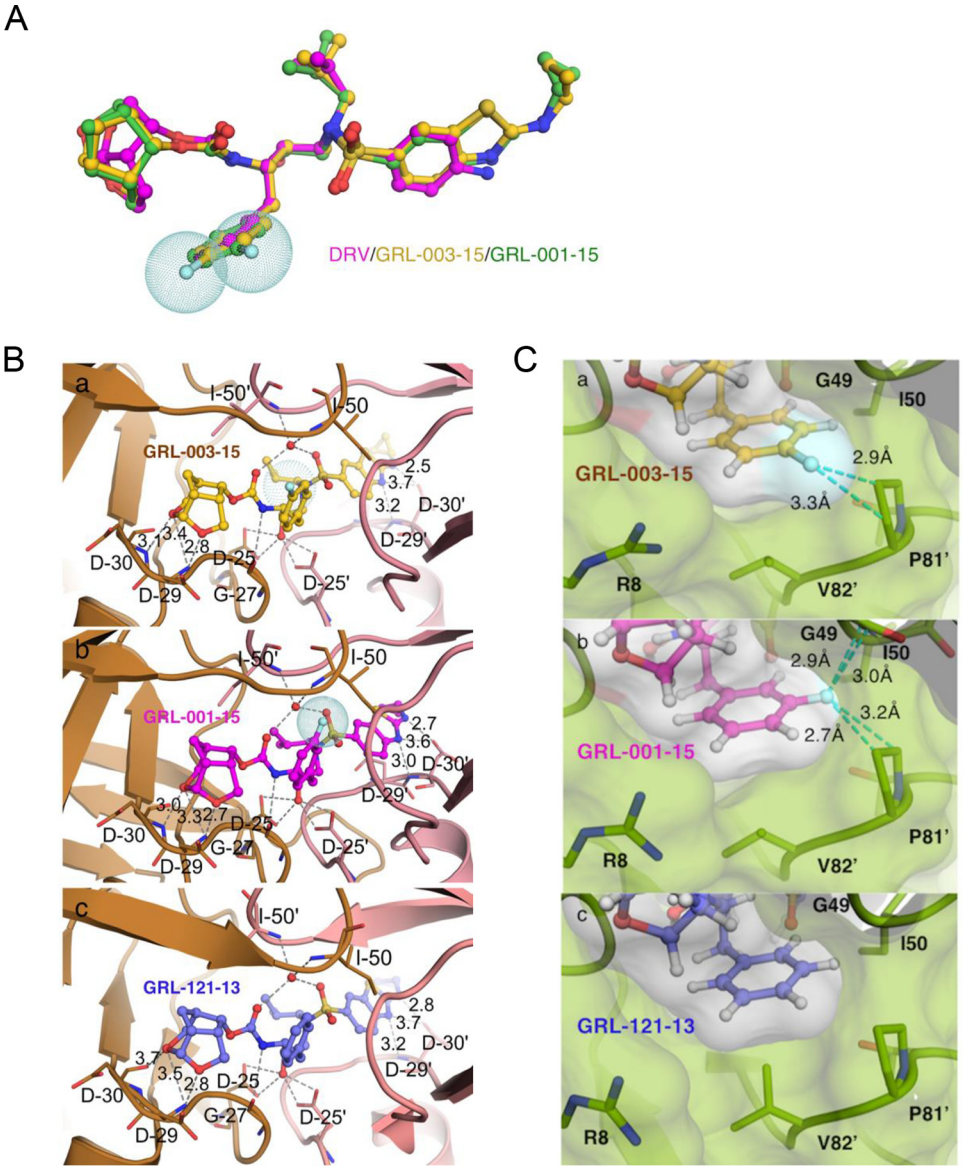


**FIG 3** X-ray crystal structure of GRL-003-15 and GRL-001-15 in the active site of wild-type HIV-1 protease. (A) Structure of DRV (magenta) overlaid with those of GRL-003-15 (yellow) and GRL-001-15 (green). All three compounds were superimposed, built on the same scaffold in the central part around the sulfonyl moiety. Note that in addition to fluorine atoms (shown as light blue-dotted spheres) attached to the P1-benzene ring, GRL-003-15 and GRL-001-15 have two moieties, P2-Crn-THF and P2′-Cp-Abt, that are larger than those of DRV. (B) Carbon atoms of GRL-003-15 (a), GRL-001-15 (b), and GRL-121-13 (c), with substitutions of HIV-PR$^{WT}$ shown in brown tones. Nitrogen, oxygen, sulfur, and fluorine atoms are shown in blue, red, yellow, and cyan, respectively. Hydrogen bond interactions of each compound with protease residues in the active site are shown by gray dashed lines. (C) Close look at fluorine atom interactions of GRL-121-13 (a), GRL-003-15 (b), and GRL-001-15 (c) inside the S1 subpocket of HIV-PR$^{WT}$. Essential fluorine-mediated interactions are shown with cyan dashed lines. The *para*-positioned fluorine from GRL-003-15, however, interacts exclusively with the P81′ ring. The *meta*-positioned fluorine from GRL-001-15 engages in halogen interactions with main chain of G49 as well as the P81′ ring. The P1 ring of GRL-121-13 does not form any interactions. Numbers with dashed lines indicate the distance (Å) of the molecular interaction.

against both HIV$_{NL4-3}$ and various PI-resistant HIV-1 variants such as $_{lab}$HIV$_{PI}^{R}$ and $_{rCL}$HIVs (Tables 1 and 2). It was also noted that both GRL-003-15 and GRL-001-15 formed very tight van der Waals interactions. As seen in Fig. 3C, the Connolly surfaces of both GRL-003-15 and GRL-001-15 were found to fairly snugly fit to the hydrophobic cavity of PR$^{WT}$. Taken together, the structural features of GRL-003-15 and GRL-001-15, forming hydrogen bonds, halogen bonds, and highly favorable van der Waals interactions with PR$^{WT}$, should directly contribute to their potent activity against HIV$_{WT}$ and various PI-resistant HIV-1 variants (Tables 1 and 2).

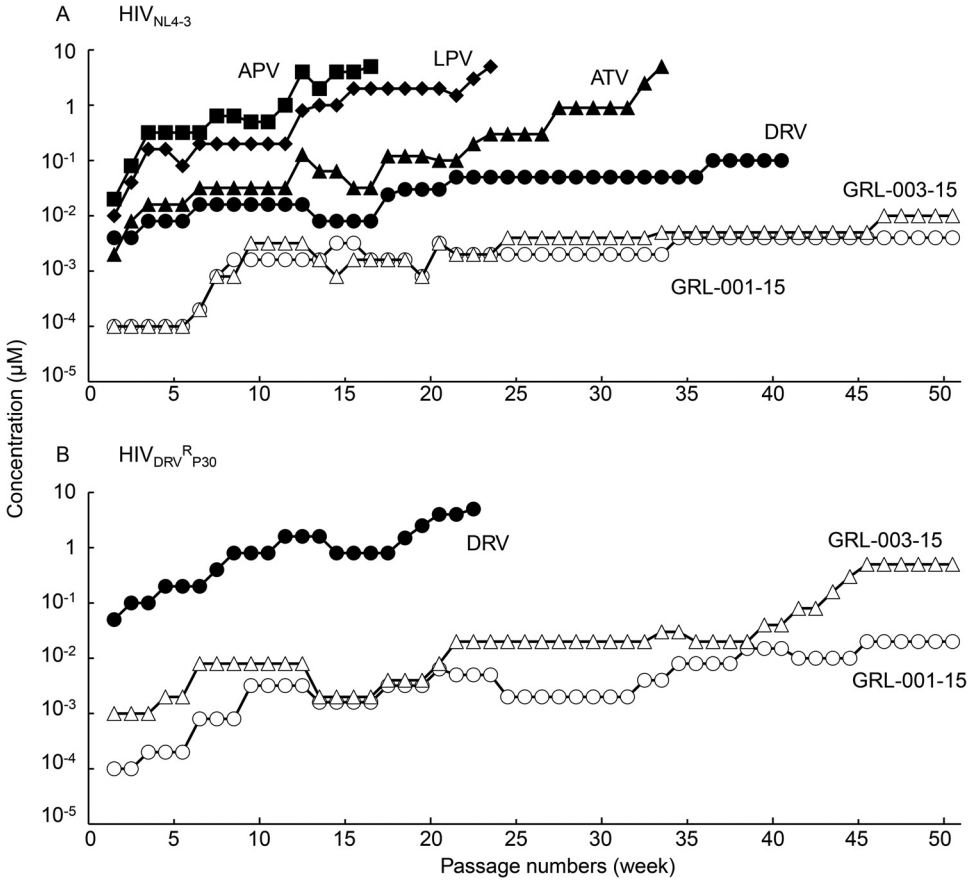


**FIG 4** *In vitro* selection of HIV-1 variants against GRL-001-15, GRL-003-15, LPV, APV, ATV, and DRV. The wild-type HIV$_{NL4-3}$ (A) and a DRV-resistant HIV-1 variant obtained from *in vitro* passage 30 with DRV (HIV$_{DRV}^{R}$$_{P30}$) (B) were propagated in the presence of increasing concentrations of each compound in MT-4 cells in a cell-free manner over 50 passages. (A) When HIV$_{NL4-3}$ was employed as a starting HIV-1 population, the virus quickly started to propagate in the presence of LPV, APV, and ATV, while DRV, GRL-001-15, and GRL-003-15 hardly allowed replication of HIV$_{NL4-3}$. (B) When HIV$_{DRV}^{R}$$_{P30}$ was employed as a starting population, the virus became highly resistant to DRV (up to 5 $\mu$M) by passage 22; however, neither HIV$_{NL4-3}$ nor HIV$_{DRV}^{R}$$_{P30}$ propagated well in the presence of GRL-001-15 or GRL-003-15 throughout the 50-week selection period.

***In vitro* selection of HIV-1 variants resistant to GRL-001-15 and GRL-003-15 using HIV-1$_{DRV}^{R}$$_{P30}$ as a starting viral population.** We then attempted to select resistant HIV-1 variants against GRL-001-15 and GRL-003-15 using the method we used in our previous studies (9, 16, 24). When we used HIV$_{NL4-3}$ as a starting viral population and propagated the virus in the presence of increasing concentrations of APV, LPV, ATV, DRV, GRL-001-15, and GRL-003-15, HIV$_{NL4-3}$ relatively quickly started to replicate despite high concentrations (up to 5 $\mu$M) of APV, LPV, and ATV. However, we failed to continuously propagate HIV$_{NL4-3}$ in the presence of DRV, GRL-001-15, and GRL-003-15 (Fig. 4A). Thus, in the second attempt at selection, we employed the highly DRV-resistant variant HIV$_{DRV}^{R}$$_{P30}$ as a starting viral population, as previously described (9, 16, 24). As we expected, with the selection pressure with DRV, the variant HIV$_{DRV}^{R}$$_{P30}$ quickly started to replicate in the presence of high concentrations of DRV (up to 5 $\mu$M) (Fig. 4B). The variant HIV$_{DRV}^{R}$$_{P30}$ hardly replicated in the presence of GRL-003-15 until 40 weeks of selection and then apparently started to propagate at a slightly greater concentration of GRL-003-15 (up to 500 nM) beyond 40 weeks, but the GRL-003-15 selection curve plateaued at 0.5 $\mu$M after 45 weeks of selection. In contrast, HIV$_{DRV}^{R}$$_{P30}$ failed to start replication throughout the 50-week period of selection with GRL-001-15, and we concluded the selection with GRL-001-15 at 0.02 $\mu$M, suggesting that GRL-001-15 had a greater genetic barrier than GRL-003-15 (Fig. 4B).

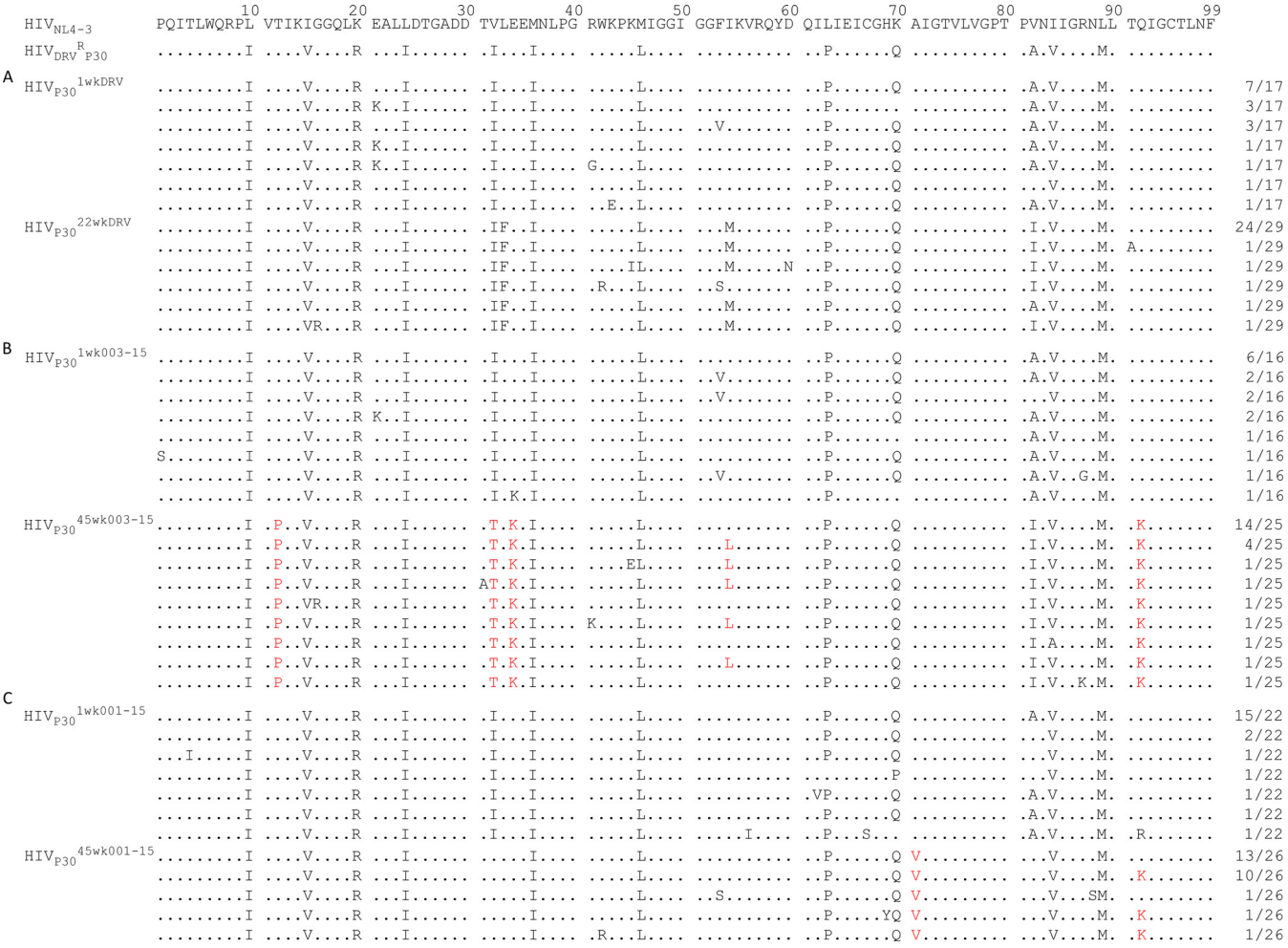


**FIG 5** Amino acid sequences of the protease of HIV-1$_{DRV}^{R}$$_{P30}$ upon selection with DRV, GRL-003-15, or GRL-001-15. The amino acid sequences deduced from the nucleotide sequences of the protease-encoding region of proviral DNA isolated from HIV$_{DRV}^{R}$$_{P30}$ selected with DRV (weeks 1 and 22) (A), GRL-003-15 (weeks 1 and 45) (B), and GRL-001-15 (weeks 1 and 45) (C) are shown. The HIV$_{NL4-3}$ and HIV$_{DRV}^{R}$$_{P30}$ amino acid sequences are displayed at the top for reference. Sequence identity at individual amino acid positions is indicated by a dot. The fractions shown on the right are the numbers of viruses that each clone is presumed to have originated from over the total number of clones examined. The unique amino acid substitutions identified in GRL-003-15- and GRL-001-15-selected HIV variants are highlighted in red.

**Reversion of key amino acid substitutions associated with HIV-1's resistance to PIs upon HIV$_{DRV}^{R}$$_{P30}$ selection with GRL-001-15.** Finally, we determined the nucleotide sequences of proviral DNA isolated from MT4 cells where HIV$_{DRV}^{R}$$_{P30}$ was selected in the presence of three PIs (DRV, GRL-003-15, and GRL-001-15) upon the termination of the indicated passage as described above. As shown in Fig. 4B, when selected with DRV, HIV$_{DRV}^{R}$$_{P30}$ continued to replicate in the presence of up to 5 $\mu$M over the 22-week selection (Fig. 4). HIV$_{DRV}^{R}$$_{P30}$ propagated over 1 week of selection with DRV (HIV$_{P30}^{1wkDRV}$) contained multiple key amino acid substitutions associated with HIV-1 resistance against DRV: V32I, V82A, and I84V (Fig. 5A) (16). However, the variant harvested at week 22 of DRV selection (HIV$_{P30}^{22wkDRV}$) had acquired three additional key amino acid substitutions related to HIV-1's resistance to DRV: L33F, I54M, and V82I. The presence of these five key amino acid substitutions and the acquisition of a high level of DRV resistance seen in HIV$_{P30}^{22wkDRV}$ are in line with our previous report (16). The variant harvested upon 1 week of selection with GRL-003-15 (HIV$_{P30}^{1wk003-15}$) contained virtually the same set of key amino acid substitutions associated with DRV resistance: V32I, V82A, and I84V. When HIV$_{DRV}^{R}$$_{P30}$ was further propagated in the presence of GRL-003-15 over an additional 44 weeks, the virus obtained (HIV$_{P30}^{45wk003-15}$) had acquired T12P, I32T, E34K, I54L, A82I, and Q92K. Two of these substitutions (T12P and E34K) are thought to be unique to the virus selected with GRL-

003-15, and the emergence of the Q92K substitution is not often seen but has been shown to be associated with the selection of $HIV_{DRV}{}^{R}{}_{P30}$ with GRL-142-13, an analogue of GRL-003-15 (24), although whether these substitutions bring about functional and/or structural alterations to $HIV_{DRV}{}^{R}{}_{P30}$ is not known at this time. The variant obtained after 1 week of selection of $HIV_{DRV}{}^{R}{}_{P30}$ with GRL-001-15 ($HIV_{P30}{}^{1wk001-15}$) also contained virtually the same set of amino acid substitutions as seen in $HIV_{P30}{}^{1wkDRV}$ and $HIV_{P30}{}^{1wk003-15}$. Interestingly, the virus harvested after 45 weeks of selection of $HIV_{DRV}{}^{R}{}_{P30}$ with GRL-001-15 ($HIV_{P30}{}^{45wk001-15}$) had lost the two major amino acid substitutions V32I and V82A, which are highly associated with HIV-1's acquisition of resistance to a variety of PIs, including DRV (9, 32–34). $HIV_{P30}{}^{45wk001-15}$ had acquired the A71V substitution in all 26 clones examined as well as Q92K in 12 of 26 clones.

## DISCUSSION

Although the progress in combined antiretroviral therapy (cART) for HIV-1 infection and AIDS has been dramatic over the decades, the emergence of HIV-1 variants that are resistant to a number of drugs in the cART regimens still limits the therapeutic options for individuals harboring such variants and remains one of the challenging issues in the long-term therapy of HIV-1/AIDS. We recently reported a novel PI, GRL-142-13, that contains a P1-2,4-*bis*-fluorophenyl moiety, P2-crown-like tetrahydropyranofuran (Crn-THF), and P2′-cyclopropyl-aminobenzothiazole and exerts highly potent activity against both $HIV_{WT}$ and $HIV_{MDR}$ variants (24, 26). Here we demonstrated that two newly designed and synthesized analogues of GRL-142-13, GRL-003-15 and GRL-001-15, which contain a fluorine atom at the *meta* and *para* positions of the P1-benzene moiety, respectively, instead of GRL-142-13's P1-2,4-*bis*-fluorophenyl moiety also exerted highly potent activity against $HIV_{WT}$ ($EC_{50}$ values of 0.057 and 0.050 nM) (Table 1). Both GRL-003-15 and GRL-001-15 also exerted potent antiviral activity against laboratory-selected multi-PI-resistant HIV-1 variants ($_{lab}HIV_{PI}{}^{R}$s) and a variety of recombinant infectious clones derived from multidrug-resistant clinical HIV-1 isolates ($_{rCL}$HIVs) (Table 2). We have previously reported that the P2 Crn-THF and cyclopropyl-aminobenzothiazole (Cp-Abt) moieties of GRL-142-13 form additional van der Waals interactions with both $PR^{WT}$ and various mutated PR species associated with high-level resistance to PIs ($PR_{PI}{}^{R}$), contributing to its unprecedentedly potent activity against various $HIV_{WT}$ and $HIV_{PI}{}^{R}$ strains (24, 35). It is most likely that the potent activity of GRL-001-15 and GRL-003-15 also stems from the presence of the P2-Crn-THF and P2′-Cp-Abt moieties in GRL-001-15 and GRL-003-15. It is of note that the positions of halogen substitutions such as fluorine atoms often affect the gain of affinity of compounds to their target(s). In general, halogen atoms larger than fluorine, such as chlorine, bromine, and iodine, require negative charges in the direction of sigma hole, while fluorine atoms are capable of interacting with other atoms, such as hydrogen atoms, with broader angles (36, 37). For this reason, whether or not the fluorine is in the *meta* or *para* position of the P1-benzene moiety in GRL-003-15 and GRL-001-15 as seen in the present study, the fluorine atom is thought to be capable of comparably forming strong halogen bond interactions.

As expected, when GRL-003-15 and GRL-001-15 were examined by differential scanning fluorimetry (DSF) using $PR^{D25N}$ (38), the thermal stability of both compounds proved to be much greater than that of DRV, strongly suggesting that both PIs tightly bind to their target protease ($PR^{D25N}$), and this tight binding of GRL-003-15 and GRL-001-15 should explain why these compounds exert much greater activity against various HIV-1 strains than DRV. GRL-121-13, whose antiviral activity was much greater than that of DRV, showed very high thermal stability compared to other three PIs, GRL-142-13, GRL-003-15, and GRL-001-15 (Fig. 2). These observations suggest that although the thermal stability of PIs can be very roughly proportionate to their anti-HIV activity, the thermal stability determined by DSF does not always exactly reflect the multitude of anti-HIV activity.

As shown in Table S1, the log *P* values of GRL-003-15, GRL-001-15, and GRL-142-13 were higher in the octanol (lipidic) interface than those of the two nonfluorinated PIs,

GRL-121-13 and DRV. The estimated values for the ionized form of the compounds (log *D*) using Tris-buffered saline (pH 7.4) were also determined. In both examinations, the values proved that the all three tested compounds were within the acceptable range for optimal lipophilicity as drug candidates (39, 40).

As depicted in Fig. 3A, superimposing the three compounds GRL-001-15, GRL-003-15, and DRV, all the compounds similarly form strong hydrogen bonds (2.7 to 3.4Å) with the protease's active-site amino acid backbones of D29 and D30. Moreover, GRL-003-15 and GRL-001-15 have two larger moieties, P2-Crn-THF and P2′-Cp-Abt, than DRV (with P2-bis-THF and P2′-aminobenzene moieties), in addition to two fluorine atoms attached to the P1-benzene ring. Thus, both GRL-003-15 and GRL-001-15 should occupy a larger space in the hydrophobic cavity within the protease dimer. These interactions of GRL-001-15 and GRL-003-15 with protease should well explain why these two compounds exert greater antiviral activity than DRV against HIV-1.

As mentioned above, the two PIs GRL-003-15 and GRL-001-15 exerted very comparable antiretroviral activity against $HIV_{WT}$ as well as $_{lab}HIV_{PI}^{R}$s and had comparable DSF features. When $HIV_{NL4-3}$ was selected in the presence of either of these PIs, the virus failed to begin propagation over 50 passages of selection (Fig. 4A), suggesting that GRL-003-15 and GRL-001-15 had a comparable genetic barrier to the emergence of HIV-1 variants. In contrast, when $HIV_{DRV}{}^{R}{}_{P30}$ was selected in the presence of GRL-003-15 or GRL-001-15, the virus selected with GRL-003-15 gradually but progressively replicated more when selected with GRL-003-15 than when selected with GRL-001-15 (Fig. 4B). The reason why we employed $HIV_{DRV}{}^{R}{}_{P30}$ as a starting HIV-1 population in this additional selection experiment is that $HIV_{DRV}{}^{R}{}_{P30}$ contains two substitutions (V32I and I84V) of the five key amino acid substitutions (V32I, L33F, I54M, V82I, and I84V) which are directly responsible for HIV-1's acquisition of high-level resistance to most of the currently available PIs, including DRV (16), and has a very high propensity to acquire the five amino acid substitutions and broad spectrum of resistance to PIs. Indeed, when $HIV_{DRV}{}^{R}{}_{P30}$ was selected with DRV, this starting virus acquired these five amino acid substitutions by 22 weeks of selection in the present study (Fig. 5A). GRL-142-13, the prototype for GRL-003-15 and GRL-001-15, contains two fluorine atoms in the 2′ and 4′ positions of the P1-benzene moiety and forms very strong halogen interactions with the amino acid residues (G49 and I50) of the flap region of protease as well as P81′, which is in the center of the hydrophobic cavity, which most likely appear to be responsible for the very high genetic barrier that GRL-142-13 retains against the emergence of resistance to GRL-142-13 (24). Our structural analyses revealed that the *meta*-positioned fluorine atom of GRL-001-15 forms bidirectional halogen bond interactions with both the G49 and P81′ residues, but GRL-003-15 completely lacks such tight binding with the flap region. GRL-142-13 also forms halogen bond interactions between another *meta*-positioned fluorine atom and the positively charged guanidium group of the R8′ residue (24). The absence of this second fluorine atom in GRL-001-15 seems to be the cause of its relatively less potent activity against various multi-PI resistant HIV-1 variants than GRL-142-13. Taken together, a structural feature of GRL-001-15, i.e., its possession of the P1-*meta*-fluorine atom, seems to confer on GRL-001-15 a more favorable genetic barrier than that of GRL-003-15.

Interestingly, when $HIV_{DRV}{}^{R}{}_{P30}$ was selected with GRL-001-15, two major amino acid substitutions (V32I and V82A) associated with high-level HIV-1 resistance to various PIs (9, 33, 41) reverted to wild-type amino acid residues, I32 and A82 (Fig. 5). The same reversion in the two amino acid substitutions had been seen when $HIV_{DRV}{}^{R}{}_{P30}$ was selected with GRL-142-13 (see Fig. S5 in reference 24. However, this reversion did not occur when $HIV_{DRV}{}^{R}{}_{P30}$ was selected with GRL-003-15, and $HIV_{DRV}{}^{R}{}_{P30}$ further acquired V82I, one of the major substitution associated with high-level resistance to multiple PIs (42, 43). Thus, it is possible that the lack of the reversion of the two major substitutions (I32 and A82) is associated with the high genetic barrier of GRL-001-15 and GRL-142-13. Moreover, the $HIV_{DRV}{}^{R}{}_{P30}$ selected with GRL-003-15 acquired four amino acid substitutions (T12P, V32T, E34K, and Q92K) by 45 weeks of selection (Fig. 5B). The role of each of these four unique substitutions is not known at this time (44, 45). In our previous

study reporting the generation of $HIV_{DRV}{}^{R}{}_{P30}$, we determined all of the Gag-encoding regions of $HIV_{DRV}{}^{R}{}_{P30}$ and other variants (16). However, a variety of amino acid substitutions were present at the outset as in the mixture of 8 highly drug-resistant clinical isolates, and more amino acid substitutions emerged under selection; therefore, we had to choose not to pursue determination of the role of each amino acid substitution in the emergence of resistance to DRV. For the same reason, we did not pursue determination of the role of each amino acid substitution in the Gag region in the present study. Pharmacokinetics studies of TMC-126, a prototype of TMC-114 (also known as DRV), with rats and dogs showed that oral bioavailability of TMC-126 was too low to warrant further clinical development (46). Further optimization of the series resulted in the selection of TMC-114 due to its superior pharmacokinetics and antiviral profile in comparison with all the other compounds of the series, such as TMC-126 (46). The aforementioned features of GRL-001-15 strongly suggest that the compound is a promising candidate as a novel anti-HIV therapeutic and that GRL-001-15 should be investigated further for potential clinical development.

## MATERIALS AND METHODS

**Cell culture and viruses.** MT-4 cells were maintained in RPMI 1640 medium containing 10% fetal calf serum (FCS), 50 U/ml penicillin, and 50 $\mu$g/ml kanamycin. The following HIV-1 strains were used for the drug susceptibility assay and selection experiments as described below: $HIV_{NL4-3}$, laboratory-selected PI-resistant HIV-1 variants ($_{lab}HIV_{PI}{}^{R}$s) ($HIV_{SQV\text{-}5\mu M}$, $HIV_{APV\text{-}5\mu M}$, $HIV_{LPV\text{-}5\mu M}$, $HIV_{IDV\text{-}5\mu M}$, $HIV_{NFV\text{-}5\mu M}$, $HIV_{ATV\text{-}5\mu M}$, and $HIV_{TPV\text{-}15\mu M}$), *in vitro*-selected DRV-resistant HIV-1 variants ($HIV_{DRV}{}^{R}$s) ($HIV_{DRV}{}^{R}{}_{P20}$, $HIV_{DRV}{}^{R}{}_{P30}$, and $HIV_{DRV}{}^{R}{}_{P51}$), and recombinant infectious clones derived from clinically isolated multidrug-resistant HIV-1 variants ($_{rCL}$HIVs) ($_{rCL}HIV_{F16}$, $_{rCL}HIV_{F39}$, $_{rCL}HIV_{V42}$, $_{rCL}HIV_{T45}$, $_{rCL}HIV_{T48}$, and $_{rCL}HIV_{F71}$). The amino acid sequences of the PI-resistant HIV-1 variants used in this study are shown in Fig. S1 in the supplemental material.

**Antiviral agents.** The nonpeptidic PIs GRL-001-15 and GRL-003-15, which contain monofluorine at the P1-phenyl moiety at the *meta* and *para* positions, respectively, were newly synthesized. The method of synthesis of these PIs will be published elsewhere. GRL-121-13 and GRL-142-13 were described previously (24, 26). Darunavir was purchased from Sigma-Aldrich.

**Drug susceptibility assay.** The susceptibility of HIV-1 to various drugs was determined as described previously (41) with minor modifications. In brief, MT-4 cells ($2 \times 10^4$ cells/ml) were exposed to various HIV-1 strains (20 ng/ml of p24) and incubated for 6 to 7 days in the presence or absence of various concentrations of drugs in 10-fold serial dilutions. Assays were performed using the Cell Counting Kit-8 (Dojindo, Japan) or the Lumipulse G1200 system with the HIV-1 p24 antigen detection kit (Fujirebio, Japan) according to the manufacturer's instructions.

**Thermal stability analysis using DSF.** A $PR^{D25N}$ solution (pH 2.8), which did not have catalytic activity, was refolded by adding 100 mM ammonium acetate (pH 6.0), which resulted in a final pH of 5.0 to 5.2. Tween 20 (0.01%) was then added to the refolded PR solution, and the solution was concentrated using Amicon Ultra-15 10K centrifugal filter units (Millipore, Darmstadt, Germany). In conducting differential scanning fluorimetry (DSF) analysis, the final concentration of each PR used was 10 $\mu$M (dimer), and the final compound concentration used was 50 $\mu$M. In the experiments, 20 mM compound solutions in dimethyl sulfoxide (DMSO) were used as stock solutions. The final buffer used contained 100 mM ammonium acetate (pH 5.0), 0.01% Tween 20, Sypro Orange (5×) (Life Technologies), 2.5% DMSO, 5 $\mu$M human renin (ProSpec-Tany TechnoGene, Ness-Ziona, Israel), and 5 $\mu$M lysozyme (Affymetrix, Santa Clara, CA). Thirty microliters of solution was successively heated from 15 to 95°C, and the changes of fluorescence intensity were documented using the 7500 Fast real-time PCR system (Applied Biosystems, Foster City, CA).

**Determination of partition and distribution coefficients of GRL-001-15 and GRL-003-15 using the shake flask method.** On day 0 of the experiment, saturation of 1-octanol [$CH_3(CH_2)_7OH$] (Nacalai Tesque, Kyoto, Japan) with distilled water and Tris-buffered saline (TBS) (10× working solution; 20 mM Tris [pH 7.4]–0.9% NaCl [Sigma-Aldrich, St. Louis, MO]) took place. Four different flasks were used. One contained 50 ml of water plus 100 ml of 1-octanol, and another contained *n*-octanol saturated with water by the addition of 50 ml of 1-octanol and 100 ml of water. For the other two flasks, the same ratios and volumes were kept for 1-octanol saturated with TBS and TBS saturated with 1-octanol. The flasks were sealed and placed in a Bioshaker at room temperature for at least 24 h at 90 rpm. Simultaneously, dilutions of GRL-001-15, GRL-003-15, GRL-121-13, GRL-142-13, and DRV were performed from a 20 mM DMSO stock solution to a final concentration of 10 $\mu$M using $H_2O$, TBS, and 1-octanol as solvents. Successive dilutions were made to obtain concentrations of 0.1, 0.05, 0.025, and 0.0125 $\mu$M. A standard curve was generated on a light spectrophotometer (Ultrospec 2100 pro; Amersham, Buckinghamshire, UK) at an absorbance of 230 nm. On day 1 of the experiment, the lipid and liquid interfaces were separated, and compounds were diluted again from 20 mM to 10 $\mu$M DMSO using 1-octanol, water, and TBS obtained from the shake flask assay. The resulting diluted compounds were then added to separate serum tubes containing equal proportions of 1-octanol and water and of 1-octanol and TBS. The solution was shaken for 5 min at 20 rpm using a tube rotator and then centrifuged at 3,500 rpm and at room temperature for 20 min. Finally, the compounds were recovered from the 1-octanol, TBS, and water interfaces and then measured on a light spectrophotometer. The values for log *P* and log *D* were

**TABLE 3** Data collection and refinement statistics using molecular replacement

| Parameter | Value[a] for: GRL-003-15_WT (PDB no. 6MCS) | GRL-001-15_WT (PDB no. 6MCR) |
|---|---|---|
| Data collection statistics | | |
| Space group | P 61 2 2 | P 61 2 2 |
| Cell dimensions | | |
| *a*, *b*, *c* (Å) | 62.51, 62.51, 82.94 | 62.78, 62.78, 82.12 |
| $\alpha$, $\beta$, $\gamma$ (°) | 90.00, 90.00, 120.00 | 90.00, 90.00, 120.00 |
| Resolution range (Å) | 32.9–21.52 (1.574–1.52) | 54.37–1.48 (1.533–1.48) |
| $R_{sym}$ or $R_{merge}$ (%) | 0.1705 (1.492) | 0.09024 (2.661) |
| $I/\sigma I$ | 9.16 (1.02) | 16.71 (1.49) |
| Completeness (%) | 99.05 (98.19) | 99.79 (99.26) |
| Redundancy (%) | 17.7 (17.8) | 18.5 (18.9) |
| Refinement statistics | | |
| Resolution range (Å) | 32.92–1.52 | 54.37–1.48 |
| No. of reflections | 15,190 (1,466) | 16,513 (1,604) |
| $R_{work}/R_{free}$ | 0.2063/0.2421 | 0.1782/0.1782 |
| No. of atoms | | |
| Total | 881 | 870 |
| Protein | 787 | 783 |
| Ligand/ion | 47 | 59 |
| Water | 47 | 28 |
| *B* factors | 28.2 | 28.88 |
| Protein | 27.66 | 28.98 |
| Ligand/ion | 31.98 | 24.39 |
| Water | 33.44 | 35.61 |
| Root mean square deviations | | |
| Bond length (Å) | 0.014 | 0.025 |
| Bond angle (°) | 1.86 | 2.11 |

[a]Values for the highest-resolution shell are shown in parentheses.

obtained according to the formulas log $P_{octanol/water}$ = log ([compound]$_{1\text{-octanol}}$/[compound]$_{water}$) and log $D_{octanol/water}$ = log ([compound]$_{1\text{-octanol}}$/[compound]$_{ionized}$ +/[compound]$_{neutral}$), where [compound]$_{1\text{-octanol}}$, [compound]$_{water}$, [compound]$_{ionized}$, and [compound]$_{neutral}$ represent the concentrations of the compound in 1-octanol, water, ionized water, and neutral water, respectively. Assays were performed following the OECD guidelines for testing of chemicals (47).

***In vitro* selection of GRL-001-15- and GRL-003-15-resistant HIV-1 variants.** We attempted to select HIV-1 variants that were resistant against GRL-003-15 and GRL-001-15 as previously described with minor modifications (16, 24). Briefly, MT-4 cells were exposed to the 50 ng/ml of p24 of $HIV_{NL4\text{-}3}$ or $HIV_{DRV^{R}P30}$ and cultured in the presence of each compound at an initial concentration equal to the $EC_{50}$. On the last day of each passage, 1 ml of the cell-free supernatant was harvested and transferred to 4 ml of culture medium containing fresh uninfected MT-4 cells in the presence of increased concentrations of the drug for the next round of culture. In this culture round, three drug concentrations (1-, 2-, and 3-fold higher than the previous drug concentration) were employed. When the replication of HIV-1 in the culture was confirmed by substantial p24 Gag protein production (increment of greater than 200 ng/ml), the highest drug concentration among the three concentrations was used to continue for the next round of culture.

**Determination of nucleotide sequences.** Molecular cloning and determination of the nucleotide sequences of HIV-1 strains passaged in the presence of each compound were performed as previously described (24) with slight modifications. In brief, DNA was extracted from HIV-1-infected MT-4 cells by using DNAzol Direct (Molecular Research Center, Cincinnati, OH) and was subjected to molecular cloning, followed by nucleotide sequence determination. Primers used for the first round of PCR with the entire Gag-PR-encoding regions of the HIV-1 genome were LTR-F1 (5′-GAT GCT ACA TAT AAG CAG CTG C-3′) and PR12 (5′-CTC GTG ACA AAT TTC TAC TAA TGC-3′). The PCR mixture consisted of 1 $\mu$l proviral DNA solution, 10 $\mu$l Premix *Taq* polymerase (Premix *Ex Taq* version 2; TaKaRa Bio Inc., Shiga, Japan), and 10 pmol of each PCR primer in a total volume of 20 $\mu$l. The PCR conditions used were an initial 1 min at 95°C, followed by 25 cycles of 30 s at 95°C, 30 s at 55°C, and 3 min at 72°C, with a final 7 min of extension at 72°C. The first-round PCR products were used directly in the second round of PCR. The second-round PCR primers used for the PR-encoding region were KAPA-1 (5′-GCA GGG CCC CTA GGA AAA AGG GCT GTT GG-3′) and Ksma2.1 (5′-CCA TCC CGG GCT TTA ATT TTA CTG GTA C-3′) under the PCR conditions of an initial 1 min at 95°C, followed by 30 cycles of 30 s at 95°C, 30 s at 55°C, and 1 min at 72°C, with a final 7 min of extension at 72°C. The PCR products were purified using spin columns (MicroSpin S-400 HR columns; GE Healthcare Life Science, Pittsburgh, PA), cloned directly using the pGEM-T Easy vector cloning system (Promega, Madison, WI), and subjected to sequencing using a model 3500 Genetic Analyzer (Applied Biosystems). The nucleotide and amino acid sequences of the protease-encoding

region of HIV variants obtained from selection of $HIV_{DRV}{}^{R}{}_{P30}$ in the presence of DRV, GRL-003-15, or GRL-001-15 are shown in Fig. S2 in the supplemental material.

**Crystallization and X-ray data collection.** Purification and crystallization of HIV-1 protease were carried out as previously described (12). Crystals of $PR^{WT}$-GRL-003-15 or -GRL-001-15 complexes were formed in 0.1 M HEPES (pH 7.5)–20% (wt/vol) polyethylene glycol 4000 – 0.2 M sodium chloride. Crystals of $PR^{WT}$-GRL-003-15 complexes were formed in 0.1 M MES (morpholineethanesulfonic acid) (pH 6.2)–15% (wt/vol) polyethylene glycol 4000 – 0.2 M lithium sulfate. X-ray data were collected at $\lambda = 1.0$ Å and 100 K at SPring-8 (Hyōgo, Japan) and processed in HKL2000 (48). Data collection statistics are shown in Table 3. The phase problem was solved by molecular replacement using Phaser (49) with the 2.0-Å structure of HIV-1 protease (PDB accession no. 5TYS) as a model. All water molecules and ligand atoms were omitted from the starting model for clarity. Subsequent cycles of refinements were performed in PHENIX (50). Coordinates and topology files for GRL-003-15 and GRL001-15 were generated using the Dundee PRODRG2 server (51) and manually fitted to the electron density. All structural figures were produced with PyMOL (version 1.3).

**Accession number(s).** X-ray crystal structures of wild-type HIV-1 protease complexed with GRL-001-15 and GRL-003-15 are available in the PDB under accession no. 6MCR and 6MCS, respectively. The nucleotide sequence data of $HIV_{P30}{}^{45wk001\text{-}15}$, $HIV_{P30}{}^{45wk003\text{-}15}$, and $HIV_{P30}{}^{22wkDRV}$ have been deposited in GenBank under accession no. MK694731, MK694732, and MK694733, respectively.

## SUPPLEMENTAL MATERIAL

Supplemental material for this article may be found at https://doi.org/10.1128/AAC.02635-18.

**SUPPLEMENTAL FILE 1**, PDF file, 0.2 MB.

## ACKNOWLEDGMENTS

The present work was supported in part by the following: the Intramural Research Program of the Center for Cancer Research, National Cancer Institute, National Institutes of Health; grants for the promotion of AIDS research from the Ministry of Health; grants from Welfare and Labor of Japan; grants for the Research Program on HIV/AIDS from the Japan Agency for Medical Research and Development (AMED) under grant numbers JP15fk0410001 and JP16fk0410101; grants from the Ministry of Education, Culture, Sports, Science, and Technology (MEXT); a grant from the National Center for Global Health and Medicine (NCGM) Research Institute (to H.M.); and a grant from the National Institutes of Health (GM53386 to A.K.G.). This work was also supported in part by the Platform Project for Supporting Drug Discovery and Life Science Research (Platform for Drug Discovery, Informatics, and Structural Life Science), funded by MEXT and AMED.

This study utilized the high-performance computational capabilities of the Biowulf Linux cluster at the National Institutes of Health, Bethesda, MD (https://hpc.nih.gov).

S.H. designed and performed antiviral assay and selection experiments and wrote the original draft. H.H. performed the protein thermal shift assay. H.H., H.B., and K.H. performed structural analysis and wrote the paper. K.V.R., P.R.N., and A.K.G. synthesized the compounds. M.A., A.K.G., and H.M. conceived the idea, designed the study, and edited final version of the manuscript. A.K.G., and H.M. supervised this project and contributed financially.

## REFERENCES

1. Katz IT, Maughan-Brown B. 2017. Improved life expectancy of people living with HIV: who is left behind? Lancet HIV 4:e324–e326. https://doi.org/10.1016/S2352-3018(17)30086-3.
2. Marcus JL, Chao CR, Leyden WA, Xu L, Quesenberry CP, Jr, Klein DB, Towner WJ, Horberg MA, Silverberg MJ. 2016. Narrowing the gap in life expectancy between HIV-infected and HIV-uninfected individuals with access To Care. J Acquir Immune Defic Syndr 73:39–46. https://doi.org/10.1097/QAI.0000000000001014.
3. Samji H, Cescon A, Hogg RS, Modur SP, Althoff KN, Buchacz K, Burchell AN, Cohen M, Gebo KA, Gill MJ, Justice A, Kirk G, Klein MB, Korthuis PT, Martin J, Napravnik S, Rourke SB, Sterling TR, Silverberg MJ, Deeks S, Jacobson LP, Bosch RJ, Kitahata MM, Goedert JJ, Moore R, Gange SJ, et al. 2013. Closing the gap: increases in life expectancy among treated HIV-positive individuals in the United States and Canada. PLoS One 8:e81355. https://doi.org/10.1371/journal.pone.0081355.
4. Teeraananchai S, Kerr SJ, Amin J, Ruxrungtham K, Law MG. 2017. Life expectancy of HIV-positive people after starting combination antiretroviral therapy: a meta-analysis. HIV Med 18:256–266. https://doi.org/10.1111/hiv.12421.
5. Cohen MS, Chen YQ, McCauley M, Gamble T, Hosseinipour MC, Kumarasamy N, Hakim JG, Kumwenda J, Grinsztejn B, Pilotto JH, Godbole SV, Chariyalertsak S, Santos BR, Mayer KH, Hoffman IF, Eshleman SH, Piwowar-Manning E, Cottle L, Zhang XC, Makhema J, Mills LA, Panchia R, Faesen S, Eron J, Gallant J, Havlir D, Swindells S, Elharrar V, Burns D, Taha TE, Nielsen-Saines K, Celentano DD, Essex M, Hudelson SE, Redd AD, Fleming TR, HPTN 052 Study Team. 2016. Antiretroviral therapy for the prevention of HIV-1 transmission. N Engl J Med 375:830–839. https://doi.org/10.1056/NEJMoa1600693.
6. Cohen MS, Chen YQ, McCauley M, Gamble T, Hosseinipour MC, Kumarasamy N, Hakim JG, Kumwenda J, Grinsztejn B, Pilotto JH, Godbole SV, Mehendale S, Chariyalertsak S, Santos BR, Mayer KH, Hoffman IF, Eshleman SH, Piwowar-Manning E, Wang L, Makhema J, Mills LA, de Bruyn G, Sanne I, Eron J, Gallant J, Havlir D, Swindells S, Ribaudo H, Elharrar V, Burns D, Taha TE, Nielsen-Saines K, Celentano D, Essex M, Fleming TR,

HPTN 052 Study Team. 2011. Prevention of HIV-1 infection with early antiretroviral therapy. N Engl J Med 365:493–505. https://doi.org/10.1056/NEJMoa1105243.
7. Joint United Nations Programme on HIV/AIDS (UNAIDS). 2018. UNAIDS data 2018. http://www.unaids.org/sites/default/files/media_asset/unaids-data-2018_en.pdf.
8. Deeks SG, Lewin SR, Ross AL, Ananworanich J, Benkirane M, Cannon P, Chomont N, Douek D, Lifson JD, Lo Y-R, Kuritzkes D, Margolis D, Mellors J, Persaud D, Tucker JD, Barre-Sinoussi F, Alter G, Auerbach J, Autran B, Barouch DH, Behrens G, Cavazzana M, Chen Z, Cohen ÉA, Corbelli GM, Eholié S, Eyal N, Fidler S, Garcia L, Grossman C, Henderson G, Henrich TJ, Jefferys R, Kiem H-P, McCune J, Moodley K, Newman PA, Nijhuis M, Nsubuga MS, Ott M, Palmer S, Richman D, Saez-Cirion A, Sharp M, Siliciano J, Silvestri G, Singh J, Spire B, Taylor J, Tolstrup M, Valente S, van Lunzen J, Walensky R, Wilson I, Zack J. 2016. International AIDS Society global scientific strategy: towards an HIV cure 2016. Nat Med 22:839–850. https://doi.org/10.1038/nm.4108.
9. Aoki M, Das D, Hayashi H, Aoki-Ogata H, Takamatsu Y, Ghosh AK, Mitsuya H. 2018. Mechanism of darunavir (DRV)'s high genetic barrier to HIV-1 resistance: a key V32I substitution in protease rarely occurs, but once it occurs, it predisposes HIV-1 to develop DRV resistance. mBio 9:e02425-17. https://doi.org/10.1128/mBio.02425-17.
10. Zazzi M. 2010. High genetic barrier antiretroviral drugs in human immunodeficiency virus-positive pregnancy. Clin Infect Dis 50:895–897. https://doi.org/10.1086/650748.
11. DHHS Panel on Antiretroviral Guidelines for Adults and Adolescents, Office of AIDS Research Advisory Council, U.S. Department of Health and Human Services. 2018. Guidelines for the use of antiretroviral agents in adults and adolescents living with HIV. https://aidsinfo.nih.gov/contentfiles/lvguidelines/AdultandAdolescentGL.pdf.
12. Hayashi H, Takamune N, Nirasawa T, Aoki M, Morishita Y, Das D, Koh Y, Ghosh AK, Misumi S, Mitsuya H. 2014. Dimerization of HIV-1 protease occurs through two steps relating to the mechanism of protease dimerization inhibition by darunavir. Proc Natl Acad Sci U S A 111:12234–12239. https://doi.org/10.1073/pnas.1400027111.
13. Koh Y, Aoki M, Danish ML, Aoki-Ogata H, Amano M, Das D, Shafer RW, Ghosh AK, Mitsuya H. 2011. Loss of protease dimerization inhibition activity of darunavir is associated with the acquisition of resistance to darunavir by HIV-1. J Virol 85:10079–10089. https://doi.org/10.1128/JVI.05121-11.
14. Koh Y, Matsumi S, Das D, Amano M, Davis DA, Li J, Leschenko S, Baldridge A, Shioda T, Yarchoan R, Ghosh AK, Mitsuya H. 2007. Potent inhibition of HIV-1 replication by novel non-peptidyl small molecule inhibitors of protease dimerization. J Biol Chem 282:28709–28720. https://doi.org/10.1074/jbc.M703938200.
15. De Meyer S, Lathouwers E, Dierynck I, De Paepe E, Van Baelen B, Vangeneugden T, Spinosa-Guzman S, Lefebvre E, Picchio G, de Bethune MP. 2009. Characterization of virologic failure patients on darunavir/ritonavir in treatment-experienced patients. AIDS 23:1829–1840. https://doi.org/10.1097/QAD.0b013e32832cbcec.
16. Koh Y, Amano M, Towata T, Danish M, Leshchenko-Yashchuk S, Das D, Nakayama M, Tojo Y, Ghosh AK, Mitsuya H. 2010. In vitro selection of highly darunavir-resistant and replication-competent HIV-1 variants by using a mixture of clinical HIV-1 isolates resistant to multiple conventional protease inhibitors. J Virol 84:11961–11969. https://doi.org/10.1128/JVI.00967-10.
17. Mitsuya Y, Liu TF, Rhee SY, Fessel WJ, Shafer RW. 2007. Prevalence of darunavir resistance-associated mutations: patterns of occurrence and association with past treatment. J Infect Dis 196:1177–1179. https://doi.org/10.1086/521624.
18. Ortiz R, Dejesus E, Khanlou H, Voronin E, van Lunzen J, Andrade-Villanueva J, Fourie J, De Meyer S, De Pauw M, Lefebvre E, Vangeneugden T, Spinosa-Guzman S. 2008. Efficacy and safety of once-daily darunavir/ritonavir versus lopinavir/ritonavir in treatment-naive HIV-1-infected patients at week 48. AIDS 22:1389–1397. https://doi.org/10.1097/QAD.0b013e32830285fb.
19. Clotet B, Bellos N, Molina JM, Cooper D, Goffard JC, Lazzarin A, Wohrmann A, Katlama C, Wilkin T, Haubrich R, Cohen C, Farthing C, Jayaweera D, Markowitz M, Ruane P, Spinosa-Guzman S, Lefebvre E, POWER 1 and 2 Study Groups. 2007. Efficacy and safety of darunavir-ritonavir at week 48 in treatment-experienced patients with HIV-1 infection in POWER 1 and 2: a pooled subgroup analysis of data from two randomised trials. Lancet 369:1169–1178. https://doi.org/10.1016/S0140-6736(07)60497-8.
20. Madruga JV, Berger D, McMurchie M, Suter F, Banhegyi D, Ruxrungtham K, Norris D, Lefebvre E, de Bethune MP, Tomaka F, De Pauw M, Vangeneugden T, Spinosa-Guzman S, TITAN Study Group. 2007. Efficacy and safety of darunavir-ritonavir compared with that of lopinavir-ritonavir at 48 weeks in treatment-experienced, HIV-infected patients in TITAN: a randomised controlled phase III trial. Lancet 370:49–58. https://doi.org/10.1016/S0140-6736(07)61049-6.
21. Kheloufi F, Allemand J, Mokhtari S, Default A. 2015. Psychiatric disorders after starting dolutegravir: report of four cases. AIDS 29:1723–1725. https://doi.org/10.1097/QAD.0000000000000789.
22. Clotet B, Feinberg J, van Lunzen J, Khuong-Josses MA, Antinori A, Dumitru I, Pokrovskiy V, Fehr J, Ortiz R, Saag M, Harris J, Brennan C, Fujiwara T, Min S, ING114915 Study Team. 2014. Once-daily dolutegravir versus darunavir plus ritonavir in antiretroviral-naive adults with HIV-1 infection (FLAMINGO): 48 week results from the randomised open-label phase 3b study. Lancet 383:2222–2231. https://doi.org/10.1016/S0140-6736(14)60084-2.
23. Zash R, Makhema J, Shapiro RL. 2018. Neural-tube defects with dolutegravir treatment from the time of conception. N Engl J Med 379:979–981. https://doi.org/10.1056/NEJMc1807653.
24. Aoki M, Hayashi H, Rao KV, Das D, Higashi-Kuwata N, Bulut H, Aoki-Ogata H, Takamatsu Y, Yedidi RS, Davis DA, Hattori SI, Nishida N, Hasegawa K, Takamune N, Nyalapatla PR, Osswald HL, Jono H, Saito H, Yarchoan R, Misumi S, Ghosh AK, Mitsuya H. 2017. A novel central nervous system-penetrating protease inhibitor overcomes human immunodeficiency virus 1 resistance with unprecedented aM to pM potency. Elife 6:e28020. https://doi.org/10.7554/eLife.28020.
25. Amano M, Miguel Salcedo-Gomez P, Yedidi RS, Delino NS, Nakata H, Venkateswara Rao K, Ghosh AK, Mitsuya H. 2017. GRL-09510, a unique P2-crown-tetrahydrofuranylurethane-containing HIV-1 protease inhibitor, maintains its favorable antiviral activity against highly-drug-resistant HIV-1 variants in vitro. Sci Rep 7:12235. https://doi.org/10.1038/s41598-017-12052-9.
26. Ghosh AK, Rao KV, Nyalapatla PR, Kovela S, Brindisi M, Osswald HL, Sekhara Reddy B, Agniswamy J, Wang YF, Aoki M, Hattori SI, Weber IT, Mitsuya H. 2018. Design of highly potent, dual-acting and central-nervous-system-penetrating HIV-1 protease inhibitors with excellent potency against multidrug-resistant HIV-1 variants. ChemMedChem 13:803–815. https://doi.org/10.1002/cmdc.201700824.
27. Niesen FH, Berglund H, Vedadi M. 2007. The use of differential scanning fluorimetry to detect ligand interactions that promote protein stability. Nat Protoc 2:2212–2221. https://doi.org/10.1038/nprot.2007.321.
28. Bright TV, Dalton F, Elder VL, Murphy CD, O'Connor NK, Sandford G. 2013. A convenient chemical-microbial method for developing fluorinated pharmaceuticals. Org Biomol Chem 11:1135–1142. https://doi.org/10.1039/c2ob27140k.
29. Liu P, Sharon A, Chu CK. 2008. Fluorinated nucleosides: synthesis and biological implication. J Fluor Chem 129:743–766. https://doi.org/10.1016/j.jfluchem.2008.06.007.
30. Karppi J, Akerman S, Akerman K, Sundell A, Nyyssonen K, Penttila I. 2007. Adsorption of drugs onto a pH responsive poly(N, N-dimethyl aminoethyl methacrylate) grafted anion-exchange membrane in vitro. Int J Pharm 338:7–14. https://doi.org/10.1016/j.ijpharm.2007.01.017.
31. Rak J, Dejlová B, Lampová H, Kaplánek R, Matějíček P, Cígler P, Král V. 2013. On the solubility and lipophilicity of metallacarborane pharmacophores. Mol Pharm 10:1751–1759. https://doi.org/10.1021/mp300565z.
32. Shafer RW. 2017. Human immunodeficiency virus type 1 drug resistance mutations update. J Infect Dis 216:S843–S846. https://doi.org/10.1093/infdis/jix398.
33. Weber IT, Agniswamy J. 2009. HIV-1 protease: structural perspectives on drug resistance. Viruses 1:1110–1136. https://doi.org/10.3390/v1031110.
34. Mahalingam B, Wang YF, Boross PI, Tozser J, Louis JM, Harrison RW, Weber IT. 2004. Crystal structures of HIV protease V82A and L90M mutants reveal changes in the indinavir-binding site. Eur J Biochem 271:1516–1524. https://doi.org/10.1111/j.1432-1033.2004.04060.x.
35. Delino NS, Aoki M, Hayashi H, Hattori SI, Chang SB, Takamatsu Y, Martyr CD, Das D, Ghosh AK, Mitsuya H. 2018. GRL-079, a novel HIV-1 protease inhibitor, is extremely potent against multidrug-resistant HIV-1 variants and has a high genetic barrier against the emergence of resistant variants. Antimicrob Agents Chemother 62:e02060-17. https://doi.org/10.1128/AAC.02060-17.
36. Zhou P, Zou J, Tian F, Shang Z. 2009. Fluorine bonding—how does it work in protein-ligand interactions? J Chem Inf Model 49:2344–2355. https://doi.org/10.1021/ci9002393.

37. Auffinger P, Hays FA, Westhof E, Ho PS. 2004. Halogen bonds in biological molecules. Proc Natl Acad Sci U S A 101:16789–16794. https://doi.org/10.1073/pnas.0407607101.
38. Sayer JM, Liu F, Ishima R, Weber IT, Louis JM. 2008. Effect of the active site D25N mutation on the structure, stability, and ligand binding of the mature HIV-1 protease. J Biol Chem 283:13459–13470. https://doi.org/10.1074/jbc.M708506200.
39. Waring MJ. 2009. Defining optimum lipophilicity and molecular weight ranges for drug candidates—molecular weight dependent lower logD limits based on permeability. Bioorg Med Chem Lett 19:2844–2851. https://doi.org/10.1016/j.bmcl.2009.03.109.
40. Ryckmans T, Edwards MP, Horne VA, Correia AM, Owen DR, Thompson LR, Tran I, Tutt MF, Young T. 2009. Rapid assessment of a novel series of selective CB(2) agonists using parallel synthesis protocols: a lipophilic efficiency (LipE) analysis. Bioorg Med Chem Lett 19:4406–4409. https://doi.org/10.1016/j.bmcl.2009.05.062.
41. Yoshimura K, Kato R, Yusa K, Kavlick MF, Maroun V, Nguyen A, Mimoto T, Ueno T, Shintani M, Falloon J, Masur H, Hayashi H, Erickson J, Mitsuya H. 1999. JE-2147: a dipeptide protease inhibitor (PI) that potently inhibits multi-PI-resistant HIV-1. Proc Natl Acad Sci U S A 96:8675–8680. https://doi.org/10.1073/pnas.96.15.8675.
42. Tie Y, Wang YF, Boross PI, Chiu TY, Ghosh AK, Tozser J, Louis JM, Harrison RW, Weber IT. 2012. Critical differences in HIV-1 and HIV-2 protease specificity for clinical inhibitors. Protein Sci 21:339–350. https://doi.org/10.1002/pro.2019.
43. Hoog SS, Towler EM, Zhao B, Doyle ML, Debouck C, Abdel-Meguid SS. 1996. Human immunodeficiency virus protease ligand specificity conferred by residues outside of the active site cavity. Biochemistry 35:10279–10286. https://doi.org/10.1021/bi960179j.
44. Mata-Munguía C, Escoto-Delgadillo M, Torres-Mendoza B, Flores-Soto M, Vázquez-Torres M, Gálvez-Gastelum F, Viniegra-Osorio A, Castillero-Manzano M, Vázquez-Valls E. 2014. Natural polymorphisms and unusual mutations in HIV-1 protease with potential antiretroviral resistance: a bioinformatic analysis. BMC Bioinformatics 15:72. https://doi.org/10.1186/1471-2105-15-72.
45. Martinez-Picado J, Savara AV, Sutton L, D'Aquila RT. 1999. Replicative fitness of protease inhibitor-resistant mutants of human immunodeficiency virus type 1. J Virol 73:3744–3752.
46. De Meyer S, Azijn H, Surleraux D, Jochmans D, Tahri A, Pauwels R, Wigerinck P, de Béthune M-P. 2005. TMC114, a novel human immunodeficiency virus type 1 protease inhibitor active against protease inhibitor-resistant viruses, including a broad range of clinical isolates. Antimicrob Agents Chemother 49:2314–2321. https://doi.org/10.1128/AAC.49.6.2314-2321.2005.
47. Organization for Economic Cooperation and Development. 1995. OECD guidlines for the testing of chemicals. Section 1, physical-chemical properties. Test no. 107. https://www.oecd.org/chemicalsafety/risk-assessment/1948169.pdf.
48. Otwinowski Z, Minor W. 1997. Processing of X-ray diffraction data collected in oscillation mode. Methods Enzymol 276:307–326. https://doi.org/10.1016/S0076-6879(97)76066-X.
49. McCoy AJ, Grosse-Kunstleve RW, Adams PD, Winn MD, Storoni LC, Read RJ. 2007. Phaser crystallographic software. J Appl Crystallogr 40:658–674. https://doi.org/10.1107/S0021889807021206.
50. Adams PD, Afonine PV, Bunkoczi G, Chen VB, Davis IW, Echols N, Headd JJ, Hung LW, Kapral GJ, Grosse-Kunstleve RW, McCoy AJ, Moriarty NW, Oeffner R, Read RJ, Richardson DC, Richardson JS, Terwilliger TC, Zwart PH. 2010. PHENIX: a comprehensive Python-based system for macromolecular structure solution. Acta Crystallogr D Biol Crystallogr 66:213–221. https://doi.org/10.1107/S0907444909052925.
51. Schuttelkopf AW, van Aalten DM. 2004. PRODRG: a tool for high-throughput crystallography of protein-ligand complexes. Acta Crystallogr D Biol Crystallogr 60:1355–1363. https://doi.org/10.1107/S0907444904011679.